

# Scaling the Size of a Formation using Relative Position Feedback <sup>★</sup>

Samuel Coogan <sup>a,★★</sup> Murat Arcaç <sup>a</sup>

<sup>a</sup>*Department of Electrical Engineering and Computer Sciences, University of California, Berkeley*

---

## Abstract

We consider a multiagent coordination problem where the objective is to steer a team of mobile agents into a formation of variable size. We assume the shape description of the formation is known to all agents, but the desired size scaling of the formation is known only to a subset of agents. We present two strategies that allow the agents to maneuver to the desired scaled formation using only local relative position information. These strategies can be implemented using information gathered via local sensors and no interagent communication. We compare the two methods through several examples with simulations.

*Key words:* Cooperative control, Autonomous mobile robots, Formation control

---

## 1 Introduction

Group coordination of mobile agents using distributed feedback laws has received increased attention as hardware and computing costs have decreased. In many cases, a team of interacting autonomous agents can accomplish tasks that are difficult or impossible for one robot to accomplish. Often, the goal of such coordination problems is to achieve global group behavior through local feedback interactions, Tsitsiklis et al. (1986), Reynolds (1987), Jadbabaie et al. (2003), Olfati-Saber & Murray (2004), Ren & Beard (2005), Olfati-Saber et al. (2007), Arcaç (2007), Yu et al. (2010).

Formation control and maintenance is a common group task and has been addressed using a variety of methods in the literature as in Tanner et al. (2003), Lawton et al. (2003), Fax & Murray (2004), Vicsek et al. (1995), Desai et al. (1998), Ogren et al. (2004), Axelsson et al. (2003), Krick et al. (2008), Hendrickx et al. (2007), Sepulchre et al. (2008), Basiri et al. (2010), and Cao et al. (2011).

Allowing some agents to be leaders and others to be

followers with unique tasks for each has also been extensively studied. To name a few, Shi & Hong (2009) discuss flocking and consensus techniques with leaders when the communication topology is time-varying and agents have nonlinear dynamics, Tanner et al. (2004) analyze stability of formation control strategies by viewing the leaders as inputs and developing a notion of leader-to-formation stability that is similar to input-to-state stability (Sontag (1989)), and Cao & Ren (2009) present a strategy for containment control using stationary or dynamic leaders with a static or time-varying directed communication topology.

In this paper, we consider the problem of formation control when only a subset of the agents, henceforth called the leaders, know the desired formation size. The remaining follower agents implement a cooperative control law using only local interagent position information such that the agents converge to the desired formation scaled by the desired size. By allowing the size of the formation to change, the group can dynamically adapt to changes in the environment such as unforeseen obstacles, adapt to changes in group objectives, or respond to threats.

We present a control strategy for the leaders and propose two strategies for the follower agents. In the first strategy, referred to as the *single link* method, each follower agent relies on one link to estimate the desired size scaling and uses a formation control law to achieve the formation. This method results in a simple geometric condition for certifying stability given a specific formation via a small-gain analysis. In the second strat-

---

<sup>★</sup> Research supported in part by the National Science Foundation under grants ECCS-0852750 and ECCS-1101876 and by the Air Force Office of Scientific Research under grant FA9550-11-1-0244. S. Coogan is supported by a National Science Foundation Graduate Research Fellowship.

<sup>★★</sup>Corresponding author Samuel Coogan. +1 510 643 2515.

*Email addresses:* [scoogan@eecs.berkeley.edu](mailto:scoogan@eecs.berkeley.edu) (Samuel Coogan), [arcaç@eecs.berkeley.edu](mailto:arcaç@eecs.berkeley.edu) (Murat Arcaç).

egy, referred to as the *multiple link* method, the follower agents calculate estimates of the desired scale along each adjacent edge. This strategy typically offers better performance in terms of speed of convergence and stability but requires a further constraint to ensure that the final formation is a scaling of the desired formation.

In both designs, we assume the agents are equipped with sensing capabilities such that relative positions of neighboring agents are available to an agent, but agents are not necessarily capable of communicating other information to one another. Such a construction may be valuable in cases where communication is expensive, unreliable, or dangerous, yet passive sensors can allow the agents to nonetheless interact with each other and accomplish a desired group behavior. Furthermore, by allowing only some nodes to determine a formation size, it may be possible to equip only these leader nodes with the potentially expensive sensing, computational, and/or communication equipment necessary for determining an appropriate formation size given factors such as environmental conditions, mission commands, etc. The follower agents could conceivably be much simpler and therefore less expensive and expendable. In addition, a fundamental understanding of what can be accomplished with relative position feedback alone is of theoretical interest in cooperative control problems.

The case of direct communication was studied in Coogan et al. (2011). A special case of the single link method in which each formation has one leader, and each follower agent employs feedback with memory to update its estimate was also studied in Coogan et al. (2011). In the present sequel, we allow multiple leaders, we consider the case in which the speed of the estimate dynamics is altered or memory in the feedback is removed altogether, and we present an alternative feedback method in which each agent monitors multiple links for the purpose of estimating the formation scale.

This paper is organized as follows: In Section 2, we introduce the problem statement. In Section 3 and Section 4, we present the single link method, and in Section 5 we present the multiple link method. We extend these methods to single integrator models and nonlinear models that are input-output linearizable in Section 6. In Section 7, we present three examples with simulations, and we summarize our main results and provide discussion in Section 8.

## 2 Problem Definition

Consider a team of  $n$  agents each represented by a position vector  $x_i \in \mathbb{R}^p$ ,  $i = 1, \dots, n$ , and assume each agent is modeled with double integrator dynamics:

$$\ddot{x}_i = f_i. \quad (1)$$

We define  $x = [x_1^T \ x_2^T \ x_3^T \ \dots \ x_n^T]^T$  and  $v = \dot{x}$  to denote the stacked vector containing the velocities of all of the agents.

We assume there is a position sensing topology by which agents are capable of inferring the relative position of other agents. We represent this topology with a *sensing* graph with  $n$  nodes representing the  $n$  agents. We assume relative position sensing is bidirectional, and if agent  $i$  and agent  $j$  have access to the quantity  $x_i - x_j$ , then the  $i$ th and  $j$ th nodes of the sensing graph are connected by an edge. We also assume that the sensing graph is connected.

Suppose there are  $m$  edges in the sensing graph. We arbitrarily assign a direction to each edge of the sensing graph and define the  $n \times m$  incidence matrix  $D$  as:

$$d_{ij} = \begin{cases} +1 & \text{if node } i \text{ is the head of edge } j \\ -1 & \text{if node } i \text{ is the tail of edge } j \\ 0 & \text{otherwise} \end{cases}$$

where  $d_{ij}$  is the  $ij$ th entry of  $D$ . Since the graph is bidirectional, this choice of direction does not affect any of the following results.

Suppose the agents are to keep a certain formation by maintaining the relative interagent displacements defined by the sensing topology. Suppose, in addition, it is allowable for the formation size to change, and a subset of the agents possess a static desired target formation scale  $\lambda^* \in \mathbb{R}$ . We call the agents in this subset *leaders* and the remaining agents *followers*. Unless otherwise stated, we assume there is at least one leader. We denote the number of leaders by  $n_l$  and the number of followers by  $n_f$ , and we assume the followers are indexed first. We thus let  $\mathcal{I}_F = \{1, \dots, n_f\}$  be the set of indices corresponding to the follower agents and  $\mathcal{I}_L = \{n_f + 1, \dots, n\}$  be the set of indices corresponding to the leader agents.

Our goal is to achieve the following group behavior:

*The relative position of two agents connected by an edge  $k$ , denoted by*

$$z_k \triangleq \sum_{i=1}^n d_{ik} x_i, \quad (2)$$

*converges to a prescribed target value  $z_k^d \lambda^*$  for each  $k = 1, \dots, m$ , i.e.,*

$$\lim_{t \rightarrow \infty} z_k = z_k^d \lambda^*, \text{ for } k = 1, \dots, m \quad (3)$$

*and*

$$\lim_{t \rightarrow \infty} v_i = 0, \text{ for } i = 1, \dots, n \quad (4)$$

*where  $v_i = \dot{x}_i$ .*

**Remark 1** For ease of exposition, we have assumed that the agents do not follow a prescribed velocity profile. If a common velocity  $v^d(t)$  is known to all the agents, then we can replace  $v$  with  $\tilde{v}(t) = v(t) - v^d(t)$  and proceed as below. See Coogan et al. (2011) for an example of how this can be achieved.

Let  $z \triangleq [z_1^T \dots z_m^T]^T = (D^T \otimes I_p)x$  and  $z^d \triangleq [(z_1^d)^T \dots (z_m^d)^T]^T$  where  $\otimes$  is the Kronecker product operator, and  $I_p$  denotes the  $p \times p$  identity matrix.

We make the following two assumptions regarding  $z^d$  to avoid ill-posedness:

- (1) We assume  $z^d \in \mathcal{R}(D^T \otimes I_p)$  where  $\mathcal{R}$  denotes range space. This requirement is necessary to ensure that there exists agent positions in  $\mathbb{R}^p$  that achieve the desired formation.
- (2) We assume  $\|z_k^d\| > 0$  for all  $k$ .

All agents have access to the static vector  $z^d$ , but only the leaders possess knowledge of  $\lambda^*$ . Thus we seek a control strategy for the leaders and the followers that achieves the desired group behavior (3)–(4), relies only on local relative position information, and does not depend on  $\lambda^*$  in the case of the followers.

Observe that our approach is a *displacement-based* algorithm and thus we require all agents to have access to a global reference frame, see Oh & Ahn (2010) for a review of formation control methods. We note that, in practice, it can be difficult to establish a global reference frame but this can be accomplished using, e.g., a global positioning system.

### 3 Formation Scaling via the Single Link Method

We introduce the following strategy for the leader agents:

$$f_i = - \sum_{j=1}^m d_{ij} (z_j - z_j^d \lambda^*) - \kappa v_i, \quad i \in \mathcal{I}_L \quad (5)$$

where  $\kappa > 0$  is a damping coefficient. Note that  $d_{ij}$  is either 0, 1, or  $-1$ , and is only nonzero when  $z_j$  is an edge connected to node  $i$ . Thus  $f_i$  in (5) is a function of only the position of neighboring agents and therefore is a distributed control strategy. Towards developing a strategy for the follower agents, we now construct a directed subgraph of the sensing graph with the following properties:

- The subgraph contains all the vertices and a (directed) subset of the edges of the sensing graph.
- Each follower node is the head of exactly one edge. The leaders are the head of no edge.
- A directed path exists to each follower node originating from a leader node.

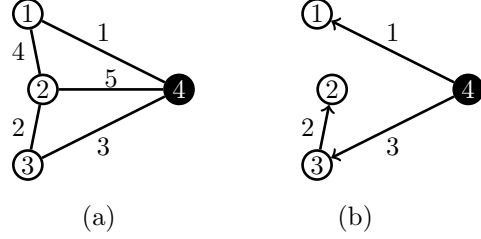


Fig. 1. (a) 4-agent, 5-edge sensing graph where agent 4 is the leader with edge indexing based on the monitoring graph. (b) One possible monitoring graph constructed from the sensing graph.

In the case of one leader, this subgraph is a directed spanning tree rooted at the leader. We call this graph the *monitoring* graph. We have assumed the follower nodes are indexed first, and without loss of generality, we now index the edges of the sensing graph such that for each edge of the monitoring graph, the index of the corresponding edge in the sensing graph matches the head node index from the monitoring graph. We arbitrarily index the remaining edges. Thus vectors  $z_1, \dots, z_{n_f}$  correspond to the monitoring edges of agents  $1, \dots, n_f$ , respectively. Fig. 1 shows an example of a formation with the sensing graph, one possible construction of the monitoring graph, and the induced edge indexing scheme.

The proposed update rule for the follower agents is

$$f_i = - \sum_{j=1}^m d_{ij} (z_j - z_j^d \lambda_i) - \kappa v_i, \quad i \in \mathcal{I}_F \quad (6)$$

where

$$\lambda_i \triangleq \frac{1}{\|z_i^d\|^2} (z_i^d)^T z_i. \quad (7)$$

This means that each follower agent  $i$  monitors one edge (edge  $i$ ) to gain a sense of the value of  $\lambda^*$  and employs (7) as an estimate. We let

$$\Delta \triangleq \begin{bmatrix} \sum_{j=1}^m d_{1j} \frac{1}{\|z_1^d\|^2} z_j^d (z_1^d)^T & & 0 \\ & \ddots & \\ 0 & & \sum_{j=1}^m d_{n_f j} \frac{1}{\|z_{n_f}^d\|^2} z_j^d (z_{n_f}^d)^T \end{bmatrix} \quad (8)$$

and

$$\tilde{z} \triangleq z - z^d \lambda^*, \quad (9)$$

and we write the strategies (5) and (6) in matrix form as

$$\dot{v} = -\kappa v - (D \otimes I_p) \tilde{z} + \begin{bmatrix} \Delta & 0 \\ 0 & 0 \end{bmatrix} \tilde{z}. \quad (10)$$

where we have used  $(D_f \otimes I_p)z^d = [\Delta \ 0]z^d$  with  $D_f$  consisting of the first  $n_f$  rows of  $D$ , i.e. we decompose  $D$  as

$$\begin{bmatrix} D_f \\ D_l \end{bmatrix} \triangleq D \quad (11)$$

where  $D_f$  includes the rows of  $D$  corresponding to the followers and  $D_l$  includes the rows corresponding to the leaders. Observing that

$$\dot{\tilde{z}} = (D^T \otimes I_p)v, \quad (12)$$

we see that we are interested in the stability of the origin of  $\begin{bmatrix} v^T & \tilde{z}^T \end{bmatrix}^T$  where the dynamics of the system are given by (10) and (12). It is easy to see that  $\mathcal{R}(D^T \otimes I_p)$  is invariant under the dynamics of (12). Furthermore,  $z^d$  is designed such that  $z^d \in \mathcal{R}(D^T \otimes I_p)$ , hence for our physical setup in which  $z$  represents relative displacement among a team of agents,  $\tilde{z}$  will evolve in the subspace  $\mathcal{R}(D^T \otimes I_p)$ .

While the stability of the overall dynamics governed by (10) and (12) can be determined using a number of techniques including direct calculation of eigenvalues, we propose a simple condition derived via application of the small-gain theorem as a certificate of stability. While this condition may be conservative, it provides an appealing geometric criterion that is easy to check using the formation geometry and eigenvalues of the graph Laplacian matrix. To this end, we consider (10) and (12) as the interconnection of two subsystems:

(1) Subsystem 1:

$$\dot{v} = -\kappa v - (D \otimes I_p)\tilde{z} + u \quad (13)$$

$$\dot{\tilde{z}} = (D^T \otimes I_p)v \quad (14)$$

$$y = \tilde{z}. \quad (15)$$

(2) Subsystem 2:

$$u = \begin{bmatrix} \Delta & 0 \\ 0 & 0 \end{bmatrix} y. \quad (16)$$

We have the following Lemmas:

**Lemma 2** Let  $\mu_1, \dots, \mu_{n-1}$  be the positive eigenvalues of the unweighted sensing graph Laplacian  $DD^T$ . Let

$$\rho_i = \begin{cases} 1/\sqrt{\mu_i} & \text{if } \kappa \geq \sqrt{2\mu_i} \\ \frac{2\sqrt{\mu_i}}{\kappa\sqrt{4\mu_i - \kappa^2}} & \text{if } \kappa < \sqrt{2\mu_i} \end{cases} \quad (17)$$

for  $i = 1, \dots, n-1$ .

The  $\mathcal{L}_2$  gain from  $u$  to  $y$  of subsystem 1 defined by (13)–(15) is

$$\gamma_1 = \max_i \{\rho_i\}. \quad (18)$$

**Proof.** We observe that the “ $\otimes I_p$ ” term only increases the multiplicity of a singular value and therefore it suffices to assume that  $p = 1$  to determine  $\gamma_1$ . Let  $D = U\Sigma V^T$  be the singular value decomposition of  $D$  with  $U \in \mathbb{R}^{n \times n}$ ,  $V \in \mathbb{R}^{m \times m}$ , and  $\Sigma \in \mathbb{R}^{n \times m}$  where  $\Sigma = \text{diag}\{\{\sqrt{\mu_i}\}_{i_0}^{n-1}\}$  and  $\{\mu_i\}_{i=0}^{n-1}$  are the eigenvalues of  $DD^T$  such that  $0 = \mu_0 < \mu_1 \leq \mu_2 \leq \dots \leq \mu_{n-1}$ . Note that if  $m = n-1$  (the minimum number of edges needed for a complete graph), then  $\sqrt{\mu_0} = 0$  is not a singular value of  $D$ , thus we have  $i_0 = 0$  if  $n \geq m$ , and  $i_0 = 1$  otherwise.

We let  $\bar{v} = U^T v$ ,  $\bar{z} = V^T \tilde{z}$  and obtain the following decoupled system after a change of basis:

$$\dot{\bar{v}} = -\kappa \bar{v} - \Sigma \bar{z} + \bar{u} \quad (19)$$

$$\dot{\bar{z}} = \Sigma^T \bar{v} \quad (20)$$

$$\bar{y} = \bar{z} \quad (21)$$

where  $\bar{u} = U^T u$  and  $\bar{y} = V^T y$ . Each decoupled system with nonzero output takes the form

$$\dot{\bar{v}}_i = -\kappa \bar{v}_i - \sqrt{\mu_i} \bar{z}_i + \bar{u}_i \quad (22)$$

$$\dot{\bar{z}}_i = \sqrt{\mu_i} \bar{v}_i \quad (23)$$

$$\bar{y}_i = \bar{z}_i \quad (24)$$

for  $i = 1, \dots, n-1$ . Each of these subsystems has transfer function

$$G_i(s) = \frac{\sqrt{\mu_i}}{s^2 + \kappa s + \mu_i}, \quad (25)$$

each with  $\mathcal{L}_2$  gain  $\rho_i$  given in (17). Using the fact that  $U$  and  $V$  are orthonormal and therefore do not alter the magnitude of the input  $u$  or the output  $y$ , the lemma follows.  $\square$

**Corollary 3** Let  $\mu_1$  denote the smallest positive eigenvalue of  $DD^T$  and  $\mu_{n-1}$  the largest. For  $\kappa \geq \sqrt{2\mu_{n-1}}$ , we have

$$\gamma_1 = \frac{1}{\sqrt{\mu_1}}. \quad (26)$$

**Lemma 4** The  $\mathcal{L}_2$  gain from  $y$  to  $u$  of subsystem 2 defined by (16) is

$$\gamma_2 = \max_{i \in \mathcal{I}_F} \left\{ \frac{\left\| \sum_{j=1}^m d_{ij} z_j^d \right\|}{\|z_i^d\|} \right\}. \quad (27)$$

**Proof.** Since  $\begin{bmatrix} \Delta & 0 \\ 0 & 0 \end{bmatrix}$  is a static matrix, it is clear that

$$\gamma_2 = \left\| \begin{bmatrix} \Delta & 0 \\ 0 & 0 \end{bmatrix} \right\|_2 \quad (28)$$

$$= \|\Delta\|_2 \quad (29)$$

which is simply the largest singular value of  $\Delta$ . Since  $\Delta$  is block diagonal, the singular values of  $\Delta$  are just the singular values of the blocks. Each block is a dyad of the form

$$\left( \sum_{j=1}^m d_{ij} z_j^d \right) \left( \frac{1}{\|z_i^d\|^2} (z_i^d)^T \right) \quad (30)$$

for  $i \in \mathcal{I}_F$ . Therefore each block has one nonzero singular value equal to the product of the norms of the column vector and the row vector which form the dyad, i.e. the nonzero singular values of  $\Delta$  are

$$\left\{ \left\| \sum_{j=1}^m d_{ij} z_j^d \right\| \cdot \frac{1}{\|z_i^d\|} \right\}, \quad i \in \mathcal{I}_F. \quad (31)$$

□

**Theorem 5** *Let  $\rho_i$  be defined as in (17). Then the control strategy (5) and (6) achieves the desired group behavior (3) and (4) if*

$$\max_i \{\rho_i\} \cdot \max_{i \in \mathcal{I}_F} \left\{ \frac{\left\| \sum_{j=1}^m d_{ij} z_j^d \right\|}{\|z_i^d\|} \right\} < 1. \quad (32)$$

**Proof.** Using Lemma 2, Lemma 4 and applying the small-gain theorem, see e.g. Khalil (2002), we conclude that without exogenous input, both  $u$  and  $y$  are  $\mathcal{L}_2$  functions. Because both subsystem 1 and subsystem 2 are linear,  $u$  and  $y$  are uniformly continuous, and, applying Barbalat's Lemma, we conclude  $y \rightarrow 0$ . □

A combination of Theorem 5 and Corollary 3 leads to the following:

**Corollary 6** *Let  $\mu_1$  be the smallest positive eigenvalue of  $DD^T$  and let  $\mu_{n-1}$  be the largest eigenvalue. If  $\kappa \geq \sqrt{2\mu_{n-1}}$  and*

$$\frac{1}{\sqrt{\mu_1}} \cdot \max_{i \in \mathcal{I}_F} \left\{ \frac{\left\| \sum_{j=1}^m d_{ij} z_j^d \right\|}{\|z_i^d\|} \right\} < 1, \quad (33)$$

*then the control strategy (5) and (6) achieves the desired group behavior (3) and (4).*

We note that when the sufficient condition above fails, stability of the single link method can be checked using other traditional approaches (eigenvalue calculation,

etc.), and the proposed algorithm still offers a novel formation control strategy.

#### 4 Adding Memory to the Scaling Estimate

We note that it is easy to add dynamics to the follower agents' estimates of the desired formation scaling without qualitatively altering the results from Section 3. This may be desirable to prevent large fluctuations in the "estimate" of  $\lambda^*$  given by (7) during transient periods when the agents may be far from the desired configuration. Suppose each follower agent possesses a dynamic local formation scalar  $\lambda_i$  for  $i \in \mathcal{I}_F$  which serves as a local estimate of  $\lambda^*$ . Define

$$\lambda \triangleq [\lambda_1 \dots \lambda_{n_f}]. \quad (34)$$

We now propose a control strategy to drive  $\lambda_i$  to  $\lambda^*$  for  $i \in \mathcal{I}_F$ . For the follower agents, let

$$f_i = - \sum_{j=1}^m d_{ij} (z_j - z_j^d \lambda_i) - \kappa v_i, \quad i \in \mathcal{I}_F \quad (35)$$

with

$$\dot{\lambda}_i = -\alpha \left( \lambda_i - \frac{(z_i^d)^T z_i}{\|z_i^d\|^2} \right), \quad i \in \mathcal{I}_F \quad (36)$$

where  $\alpha \in (0, \infty)$ . To write the system in block form, define the following:

$$\Delta_1 \triangleq \begin{bmatrix} \sum_{j=1}^m d_{1j} z_j^d & 0 \\ & \ddots \\ 0 & \sum_{j=1}^m d_{n_f j} z_j^d \end{bmatrix} \quad (37)$$

$$\Delta_2 \triangleq \begin{bmatrix} \frac{1}{\|z_1^d\|^2} (z_1^d)^T & 0 \\ & \ddots \\ 0 & \frac{1}{\|z_{n_f}^d\|^2} (z_{n_f}^d)^T \end{bmatrix}. \quad (38)$$

We can then write (5), (35), and (36) in matrix form as

$$\dot{v} = -\kappa v - (D \otimes I_p) \tilde{z} + \begin{bmatrix} \Delta_1 \\ 0_{n_1 p \times n_f} \end{bmatrix} \tilde{\lambda} \quad (39)$$

$$\dot{\tilde{z}} = (D^T \otimes I_p) v \quad (40)$$

$$\dot{\tilde{\lambda}} = -\alpha \tilde{\lambda} + \begin{bmatrix} \Delta_2 & 0_{n_f \times (m-n_f)p} \end{bmatrix} \tilde{z} \quad (41)$$

where we shift the equilibrium to the origin by defining  $\tilde{\lambda} = \lambda - \lambda^* \mathbf{1}$ . We depict system (39)–(41) as the interconnection of two subsystems as in Fig 2.

We again apply the small-gain theorem to these two subsystems to determine the stability of (39)–(41). Observing that the  $H_\infty$  gain of the lower subsystem is obtained

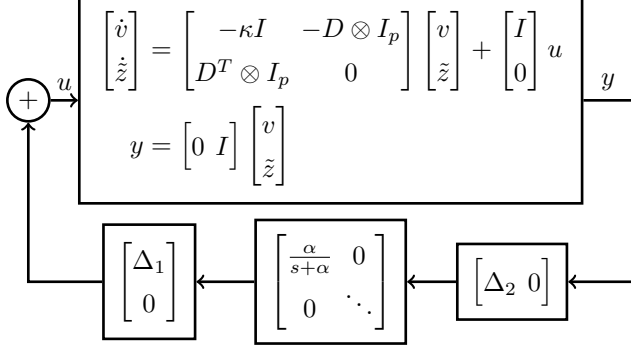


Fig. 2. System (39)–(41) as the interconnection of two sub-systems.

when  $s = 0$  and that  $\Delta_1 \Delta_2 = \Delta$ , we obtain the following lemma:

**Lemma 7** *The  $\mathcal{L}_2$  gain from  $y$  to  $u$  of*

$$u = \begin{bmatrix} \Delta_1 \\ 0 \end{bmatrix} \begin{bmatrix} \frac{\alpha}{s+\alpha} & 0 \\ 0 & \ddots \end{bmatrix} \begin{bmatrix} \Delta_2 & 0 \end{bmatrix} y \quad (42)$$

is

$$\gamma_2 = \max_{i \in \mathcal{I}_F} \left\{ \frac{\left\| \sum_{j=1}^m d_{ij} z_j^d \right\|}{\|z_i^d\|} \right\}. \quad (43)$$

Substituting Lemma 7 for Lemma 4, we see that Theorem 5 and Corollary 6 still hold if the followers use  $\lambda$  update rule (36) with control strategy (35).

## 5 Formation Scaling via the Multiple Link Method

We again assume that the leader agents use strategy (5). We define

$$\lambda_j \triangleq \frac{1}{\|z_j^d\|^2} (z_j^d)^T z_j \quad (44)$$

and propose the following strategy for the follower agents:

$$f_i = - \sum_{j=1}^m d_{ij} (z_j - z_j^d \lambda_j) - \kappa v_i, \quad i \in \mathcal{I}_F. \quad (45)$$

The difference between (45) and (6) is that in (45), the estimate of  $\lambda^*$  changes for each link within the summation, whereas in (6), one link was assigned to each agent in order to estimate  $\lambda^*$ . Let

$$P_j \triangleq \frac{1}{\|z_j^d\|^2} z_j^d (z_j^d)^T \quad (46)$$

be the orthogonal projection matrix onto

$$S_j \triangleq \text{span}\{z_j^d\} \subset \mathbb{R}^p. \quad (47)$$

Let

$$Q_j = I_p - P_j \quad (48)$$

be the orthogonal projection onto  $S_j^\perp$  where  $^\perp$  denotes orthogonal complement. Also let

$$P \triangleq \begin{bmatrix} P_1 & & 0 \\ & \ddots & \\ 0 & & P_m \end{bmatrix} \quad (49)$$

$$Q \triangleq I_{pm} - P, \quad (50)$$

observing that  $P$  is the orthogonal projection matrix onto

$$S \triangleq S_1 \times \cdots \times S_m = \prod_{j=1}^m S_j \subset \mathbb{R}^{mp} \quad (51)$$

and  $Q$  is the orthogonal projection onto  $S^\perp$ . Let

$$D_Q \triangleq \begin{bmatrix} (D_f \otimes I_p) Q \\ (D_l \otimes I_p) \end{bmatrix}. \quad (52)$$

Then we can rewrite (45) as

$$f_i = - \sum_{j=1}^m d_{ij} Q_j z_j - \kappa v_i, \quad i \in \mathcal{I}_F. \quad (53)$$

Observing that  $Q z^d = 0$ , we can combine the leader and follower strategies and write (5) and (45) in matrix form as

$$\dot{v} = -D_Q \tilde{z} - \kappa v. \quad (54)$$

We first explore the case in which we do not have any leaders, which is interesting in its own right and offers insight into the geometric requirements for ensuring that the scaled formation is attained.

**Lemma 8** *Suppose there are no leader agents, i.e.  $D_Q = (D \otimes I_p) Q$ . Then strategy (53) asymptotically converges to a scaling of the desired formation  $z^d$  for all initial conditions if and only if*

$$\mathcal{R}(D^T \otimes I_p) \cap S = \text{span}\{z^d\}. \quad (55)$$

**Proof.** With no leaders, we let  $\lambda^* = 0$  without loss of generality and then  $z = \tilde{z}$ .

(if) Let  $V \triangleq \frac{1}{2}(v^T v + z^T Q z)$  be a Lyapunov function for the system. Recalling that  $\dot{z} = (D^T \otimes I_p)v$ , we have  $\dot{V} = -\kappa v^T v \leq 0$ . Applying LaSalle's principle, we see

that  $v \equiv 0$  only if  $(D \otimes I_p)Qz = 0 \implies Qz \in \mathcal{N}(D \otimes I_p)$ . But also  $z \in \mathcal{R}(D^T \otimes I_p) = \mathcal{N}(D \otimes I_p)^\perp$ . Therefore, if  $v \equiv 0$ , we have  $\|Qz\|^2 = z^T Q^T Qz = z^T (Qz) = 0$ , and thus  $z \in \mathcal{N}(Q) = S$ . By condition (55), we have  $z \in \text{span}\{z^d\}$ .

(only if) If we assume that condition (55) does not hold, then there exists a  $z^*$  such that  $z^* \in \mathcal{R}(D^T \otimes I_p) \cap S$  and  $z^* \notin \text{span}\{z^d\}$ . Since  $z^* \in S$  and  $Q$  is the orthogonal projection onto  $S^\perp$ ,  $Qz^* = 0$  and therefore  $v = 0$ ,  $z = z^*$  is an equilibrium of (53), but  $z^*$  is not a scaling of the desired formation.  $\square$

Via the proof of Lemma 8, we see that strategy (45) ensures that  $\lim_{t \rightarrow \infty} z \in S$ , i.e. that each edge specified in the formation obtains the correct direction in the limit. Thus, to ensure that a scaling of the desired formation is obtained, we must ensure that if all formation edges  $z_j$  are constrained to have the prescribed direction of  $z_j^d$ , then it must be that all edges have the same scaling of  $z_j^d$ , and this condition is captured explicitly in (55). A formation specification satisfying this condition is said to be *parallel rigid* and has been studied primarily in the computer-aided design literature, see e.g. Servatius & Whiteley (1999). If  $z$  is such that  $z \in \mathcal{R}(D^T \otimes I_p) \cap S$ , then  $z$  is said to be a *parallel redrawing* of  $z^d$ , and  $z$  is a *trivial parallel redrawing* if  $z = \alpha z^d$  for some  $\alpha \in \mathbb{R}$ . Thus a formation is parallel rigid (i.e. satisfies (55)) if and only if all parallel redrawings are trivial. There exists a duality between the concepts of parallel rigidity and the more standard distance-based rigidity, see Eren (2007) and Eren et al. (2004) for details.

**Theorem 9** *With at least one leader, the control strategy (5) for the leaders and the multiple link method (45) for the followers achieves the desired group behavior (3)–(4) for sufficiently large  $\kappa$  if and only if the equilibrium subspace  $\mathcal{R}(\mathbf{1}^T \otimes I_p)$  of the auxiliary system*

$$\dot{\xi} = -D_Q(D^T \otimes I_p)\xi \quad (56)$$

is asymptotically stable.

**Proof.** We consider the asymptotic stability of the origin of

$$\dot{v} = -\kappa v - D_Q \tilde{z} \quad (57)$$

$$\dot{\tilde{z}} = (D^T \otimes I_p)v. \quad (58)$$

(if) Let

$$A = \begin{bmatrix} -\kappa I_{np} & -D_Q \\ (D^T \otimes I_p) & 0_{mp \times mp} \end{bmatrix}. \quad (59)$$

We have that the system (57)–(58) evolves in the sub-

space  $\tilde{z} \in \mathcal{R}(D^T \otimes I_p)$ , thus  $\mathcal{R}(W)$  with

$$W = \begin{bmatrix} I & 0 \\ 0 & D^T \otimes I_p \end{bmatrix} \quad (60)$$

is an  $A$ -invariant subspace. Rather than investigate the dynamics of (57)–(58) directly, we can instead consider the dynamics in this  $A$ -invariant space. To this end, note that  $AW = WC$  with

$$C = \begin{bmatrix} -\kappa I & -D_Q(D^T \otimes I_p) \\ I & 0 \end{bmatrix}. \quad (61)$$

Thus, we can consider the stability properties of

$$\dot{\eta} = C\eta, \quad (62)$$

keeping in mind that

$$\mathcal{N}(C) = \mathcal{N}(W) = \mathcal{R}\left(\begin{bmatrix} 0 & (\mathbf{1}^T \otimes I_p) \end{bmatrix}^T\right) \quad (63)$$

is nontrivial. In particular, (57)–(58) restricted to the subspace  $\mathcal{R}(W)$  is asymptotically stable if and only if the equilibria subspace  $\mathcal{N}(W)$  of (62) is asymptotically stable. Via block matrix inversion formulae using Schur complements, we have that the characteristic polynomial of  $C$  is

$$\begin{aligned} \det(sI - C) &= \det(s^2 I + \kappa s I + D_Q(D^T \otimes I_p)) \quad (64) \\ &= \prod_{i=1}^{mp} (s^2 + \kappa s - \mu_i(-D_Q(D^T \otimes I_p))) \end{aligned} \quad (65)$$

where  $\mu_i(-D_Q(D^T \otimes I_p))$  is the  $i$ th eigenvalue of  $-D_Q(D^T \otimes I_p)$ . Thus each eigenvalue of  $-D_Q(D^T \otimes I_p)$  generates two eigenvalues of  $C$ , specifically

$$\mu_{i+,i-} = \frac{-\kappa \pm \sqrt{\kappa^2 + 4\mu_i(-D_Q(D^T \otimes I_p))}}{2}. \quad (66)$$

In general,  $\text{Re}[\mu_i] < 0$  does not imply  $\text{Re}[\mu_{i+,i-}] < 0$ , however this implication is true if

$$\kappa > \sqrt{\frac{\text{Im}[\mu_i]^2}{|\text{Re}[\mu_i]|}}. \quad (67)$$

By assumption,  $-D_Q(D^T \otimes I_p)$  has  $p$  eigenvalues at 0 and the rest are in the open left half plane. Thus, if  $\kappa$  satisfies (67) for all nonzero  $\mu_i$ , then the  $p$  zero eigenvalues of  $-D_Q(D^T \otimes I_p)$  will generate  $p$  zero eigenvalues of  $C$

corresponding to the equilibria subspace  $\mathcal{N}(W)$ , and the remaining eigenvalues will be in the open left half plane.

(only if) Via (66), it is clear that if  $\text{Re}[\mu_i] \geq 0$ , then this  $\mu_i$  corresponds to an eigenvalue of (59) with real part greater than or equal to zero. Thus if (56) has additional unstable modes, this will correspond to unstable modes of (59).

□

When we introduce leaders, (55) is no longer a necessary condition for stability and is thus not an assumption in Theorem 9, but we can modify (55) slightly and obtain the following necessary condition:

*With at least one leader, the following is a necessary condition for the system defined by (54) and (12) to achieve the desired group behavior (3)–(4):*

$$\mathcal{R}(D^T \otimes I_p) \cap S \cap \mathcal{N}(D_l \otimes I_p) = \{\mathbf{0}\}. \quad (68)$$

Thus, we see that (55) is most valuable as a design tool for use with the multiple link method as is seen in the following corollary:

**Corollary to Lemma 8** *If (55) is satisfied for the case with no leaders, then converting at least one follower to a leader removes  $(\bar{z} \in \text{span}\{z^d\}, v = \mathbf{0})$  from the equilibrium subspace of (54) and (12) for almost all desired formations  $z^d$  (i.e., except a set of measure zero).*

**Proof.** First, observe that there exists some  $\bar{z} \in \mathcal{R}(D^T \otimes I_p)$  such that  $(D_l \otimes I_p)\bar{z} \neq \mathbf{0}$ : if not, then  $(D_l \otimes I_p)(D^T \otimes I_p)\xi = \mathbf{0}$  for all  $\xi$ , which implies  $(D_l D_l^T \otimes I_p)\eta = \mathbf{0}$  for all  $\eta$ , which is a contradiction since it is easily verified that  $D_l D_l^T > 0$  for connected graphs. Thus  $\mathcal{N}(D_l \otimes I_p) \cap \mathcal{R}(D^T \otimes I_p)$  is a proper subspace of  $\mathcal{R}(D^T \otimes I_p)$  and therefore the set of  $\xi$  such that  $(D_l D^T \otimes I_p)\xi = \mathbf{0}$  has zero (Lebesgue) measure. Applying Lemma 8 and (68) gives the result. □

The corollary shows that (61) and its geometric interpretation should be interpreted as a design methodology for designing desired formations. However, introducing leaders may create instabilities, thus we have Theorem 9. □

## 6 Extensions to Other Agent Models

### 6.1 Single Integrator Agent Models

Suppose agent  $i$  is modeled as a single integrator agent, i.e.

$$\dot{x}_i = f_i \quad (69)$$

where we now consider the same control strategies (5) and (6) with  $\kappa = 0$  (i.e., no velocity damping). The single link method and the multiple link method then result in the following dynamics:

(1) Single link method:

$$\dot{x} = -(DD^T \otimes I_p)x + u \quad (70)$$

$$y = (D^T \otimes I_p)x \quad (71)$$

$$u = \begin{bmatrix} \Delta & 0 \\ 0 & 0 \end{bmatrix} y. \quad (72)$$

(2) Multiple link method:

$$\dot{x} = -(D_Q(D^T \otimes I_p))x. \quad (73)$$

We have again written the single link method as the interconnection of two subsystems so we can easily apply the small-gain theorem. Indeed, we have the following lemma:

**Lemma 10** *The  $\mathcal{L}_2$  gain of*

$$\dot{x} = -(DD^T \otimes I_p)x + u \quad (74)$$

$$y = (D^T \otimes I_p)x \quad (75)$$

is

$$\gamma_2 = \frac{1}{\sqrt{\mu_1}} \quad (76)$$

where  $\mu_1$  is the second smallest eigenvalue of the graph Laplacian  $DD^T$ , known as the Fiedler eigenvalue or the algebraic connectivity of the sensing graph.

The proof is similar to that of Lemma 2 and is omitted.

Using Lemma 10, Lemma 4, and the small-gain theorem, we see that condition (33) of Corollary 6 ensures that the single link method applied to single integrator models achieves the desired group behavior (3) and (4).

In the case of the multiple link method, we observe that system (73) is identical to the auxiliary system (56) in Theorem 9. Thus we see a formation resulting in stable dynamics for double integrator dynamics also results in stable dynamics when applied to single integrator models.

### 6.2 Input-Output Linearizable Agent Models

Suppose each agent  $i$  has a model of the form

$$\dot{\zeta}_i = f^i(\zeta_i) + g^i(\zeta_i)u_i \quad (77)$$

$$v_i = h^i(\zeta_i) \quad (78)$$

$$\dot{x}_i = v_i \quad (79)$$



where  $\zeta_i \in \mathbb{R}^{q_i}$  for some  $q_i \geq p$ ,  $u_i \in \mathbb{R}^p$  is the input, and  $v_i \in \mathbb{R}^p$  is the output. Further suppose the agent models have *vector relative degree*  $[1 \dots 1]$  with respect to  $v_i$ , see e.g. Sastry (1999).

Note that the dynamics (77)–(78) do not depend on  $x_i$ . This captures the intuitive notion that, for most physically relevant systems in which we identify  $x_i$  with position, the internal dynamics will not depend on the absolute position of the agent. The double integrator dynamics of (1) are a special case of (77)–(79) in which  $f^i(\zeta_i) \equiv 0$ ,  $g^i(\zeta_i) \equiv 1$ , and  $h^i(\zeta_i) = \zeta_i$ .

After input-output linearization, it is possible to bring each system into the form

$$\dot{v}_i = \ddot{x}_i = w_i \quad (80)$$

with zero dynamics defined by

$$\dot{\eta}_i = f_0^i(\eta_i, \xi_i) \quad (81)$$

where  $w_i$  is the (new) input,  $\eta_i \in \mathbb{R}^{q_i-p}$ ,  $\xi_i \in \mathbb{R}^p$ , and  $\eta_i, \xi_i$  are the state variables after a change of coordinates, i.e.  $\begin{bmatrix} \eta_i^T & \xi_i^T \end{bmatrix}^T = T_i(\zeta_i)$  with  $T_i(\cdot)$  a diffeomorphism.

If the single link method or the multiple link method is stable in the case considered in Sections 3 and 5, then the same strategy with  $w_i$  as input results in exponential stability of the origin for the system (80) with state  $\begin{bmatrix} v^T & \tilde{z}^T \end{bmatrix}^T$  where, as before,  $\tilde{z} = (D^T \otimes I_p)x - \lambda^* z^d$ . Thus, if the origin of the zero dynamics  $\dot{\eta}_i = f_0^i(\eta, 0)$  is also asymptotically stable for each  $i$ , i.e. each system is minimum phase, then the system dynamics are locally asymptotically stable. Global stability results can be obtained under more restrictive conditions on the zero dynamics such as *input-to-state stability* of (81) with respect to input  $\xi_i$ , Sontag (1989).

## 7 Simulation Results

*Example 1. Single link method with scaling estimate memory.*

Consider the formation in the plane depicted in Fig. 1(a) where the direction of each edge is arbitrary,  $D$  corresponds to the chosen node and edge numbering and direction assignment, agent 4 is the leader, and the monitoring subgraph is shown in Fig. 1(b). We let

$$z^d = \begin{bmatrix} -1 & 0.5 & 0.1 & 0.5 & -1 & -0.5 & 0.1 & -0.5 & 0.9 & 0 \end{bmatrix}^T, \quad (82)$$

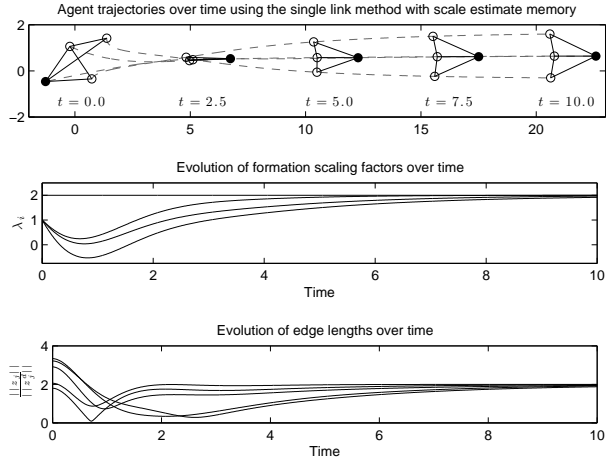


Fig. 3. Simulation results for a 4-agent, 5-edge formation using the single link method with formation scale estimate memory. The shaded node indicates the leader.

which is consistent with the shape depicted in Fig. 1(a). We have that  $\mu_1 = 2$  is the smallest positive eigenvalue of  $DD^T$  and  $\mu_3 = 4$  is the largest eigenvalue of  $DD^T$ . Now suppose we implement the control strategy (35) with  $\lambda$  update rule (36). If  $\kappa \geq \sqrt{8}$ , then, by Corollary 3,

$$\gamma_1 \leq \frac{1}{\sqrt{2}}. \quad (83)$$

Using the geometric condition presented in Lemma 7 we have that  $\gamma_2 = 1.373$ . Thus

$$\gamma_1 \gamma_2 = 1.373 \frac{1}{\sqrt{2}} = 0.971 < 1 \quad (84)$$

and therefore the system achieves the desired group behavior by Theorem 5 and its corollary. Fig. 3 shows simulation results for this case with  $\lambda^* = 2$ ,  $\lambda_i(0) = 1$  for  $i = 1, \dots, n_f$ ,  $\alpha = 1$ , and the agents' initial positions initialized randomly.

*Example 2. Dynamic desired formation scale.*

While the results derived in this paper assume a static  $\lambda^*$ , it is clear that if  $\lambda^*$  does not change quickly or often with respect to the formation dynamics, then the desired scaling can be used to dynamically adjust the formation over time. We demonstrate this using the multiple link method in Figure 4. The formation is initialized so that  $z(0) = z^d(0)$  with  $\lambda^*(t) = \begin{cases} 2, & t \in [0, 7.5) \\ 0.75, & t \in [7.5, 15]. \end{cases}$

*Example 3. Comparison of methods when condition (55) is and is not satisfied.*

Consider the regular pentagon formation depicted in Fig. 5(a) with monitoring subgraph depicted in Fig. 5(b).

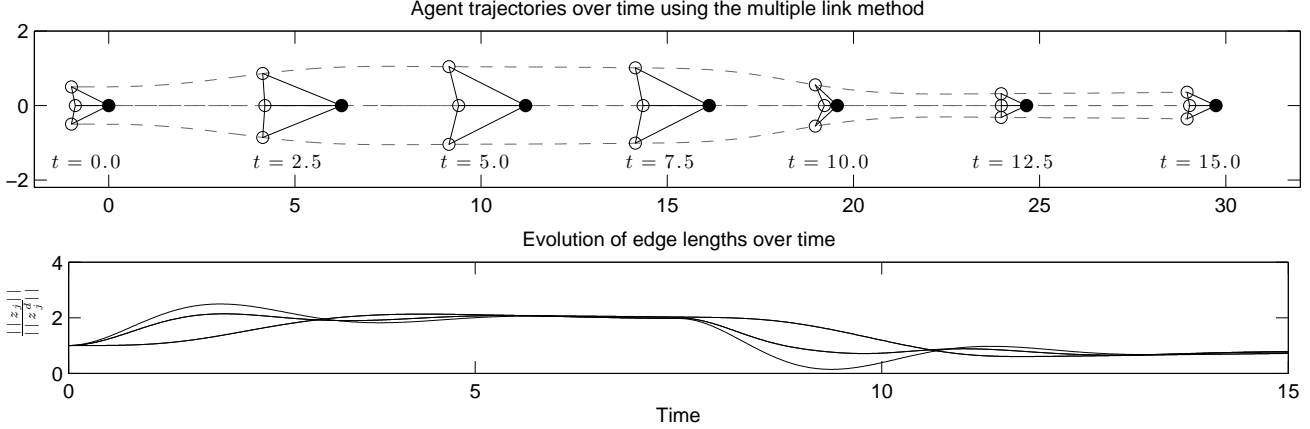


Fig. 4. Simulation results for a 4-agent, 5-edge formation using the multiple link method in which the agents are initialized in the correct formation such that  $z(0) = z^d(0)$  and  $\lambda^* = 2$  on  $t \in [0, 7.5]$  and  $\lambda^* = 0.75$  on  $t \in [7.5, 15]$ . The shaded node indicates the leader.

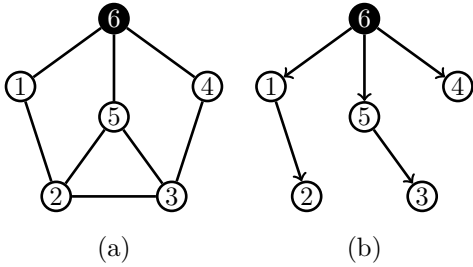


Fig. 5. (a) Regular pentagon formation with (b) monitoring subgraph where agent 6 is the leader.

This example formation does not satisfy (55). Indeed, Fig. 6 shows that, while both methods are stable, the multiple link method does not reach the desired scaled formation. The plot of  $\frac{\|z_j\|}{\|z_j^d\|}$  shows that the lengths of the edges does not converge to a common value reflecting the fact that the subspace  $\mathcal{R}(D^T \otimes I_p) \cap \mathcal{S}$  has dimension larger than one. By adding edges between nodes 1 and 5 and nodes 4 and 5 to the desired formation, condition (55) is satisfied and (3)–(4) is achieved. Figure 7 shows that both methods converge to the desired formation in this case. In Fig. 6 and 7, the simulation using the single link method does not use scale estimate memory.

We note that the regular pentagon and monitoring graph depicted in Fig. 5 do not satisfy (33) because the product of the  $\mathcal{L}_2$  gains is 1.892. Therefore Theorem 5 cannot be used to certify stability, however the formation control strategy is indeed stable as can be clearly seen in the simulations and verified by inspecting the eigenvalues of the closed loop system. Thus the single link method still offers a novel formation control approach.

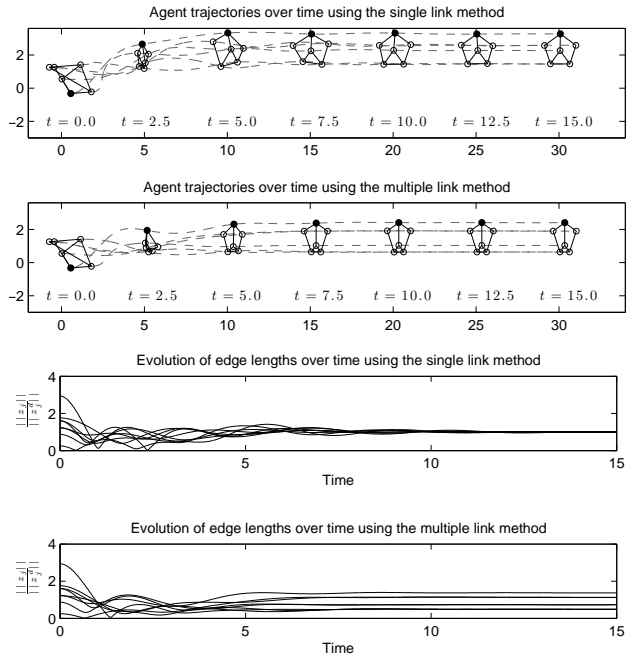


Fig. 6. Simulation results for a 6-agent, 8-edge formation that does not satisfy (55). The shaded node is the leader.

## 8 Conclusions

In this paper, we introduce increased flexibility and adaptivity to the standard formation maintenance problem by presenting cooperative control strategies that allow a multiagent team to dynamically alter its formation size while only requiring relative position information. To address interagent collisions or collisions with the environment, we note that low level collision avoidance controllers can be incorporated which are inactive or have negligible effect when agents are not at risk of colliding. In addition, the leaders could poten-

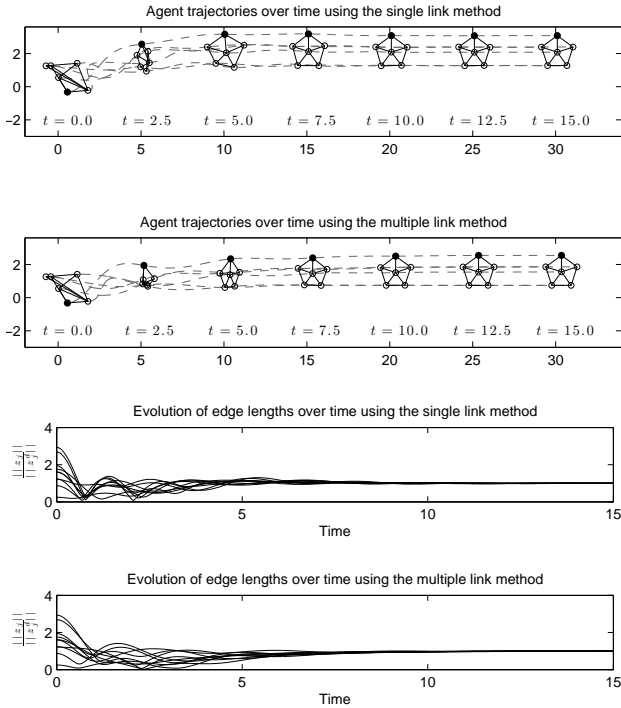


Fig. 7. Simulation results for a 6-agent, 10-edge formation that satisfies (55). The shaded node is the leader.

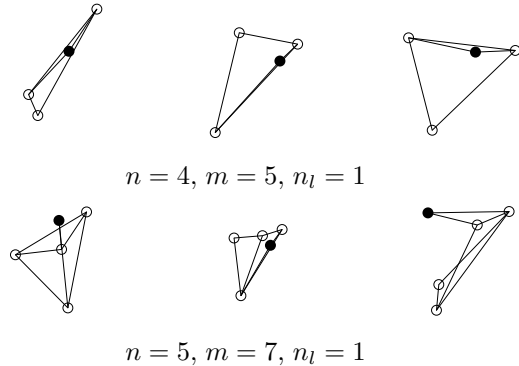


Fig. 8. Formations that result in unstable dynamics with the multiple link method. The shaded node indicates the leader agent.

tially avoid collision with environmental obstacles by altering the formation size.

For the single link method, we have presented an easily verified sufficient condition for stability derived via the small-gain theorem. While such a geometric condition for stability does not exist for the multiple link method, we remark that, qualitatively, the multiple link method offers superior performance in terms of speed of convergence and stability as observed in simulation. In addition, we observe that formations which tend to be unstable when used with the multiple link method are for-

mations in which three or more agents are very nearly colinear, a condition which can often be avoided when designing the desired formation. Fig. 8 shows several unstable formation shapes with one leader for varying  $n$  and  $m$  that fail Theorem 9 because the corresponding auxiliary system (56) is unstable.

A number of interesting directions for future research remain. For example, we assume the sensing topology is fixed. It may be more practical for the sensing topology to be time-varying according to the sensing properties of the agents. Additionally, rather than requiring the agents' velocities to decay to zero, we could allow the agents to agree on a constant but nonzero velocity.

## References

- Arcak, M. (2007). Passivity as a design tool for group coordination. *IEEE Transactions on Automatic Control*, 52, 1380–1390.
- Axelsson, H., Muhammad, A., & Egerstedt, M. (2003). Autonomous formation switching for multiple, mobile robots. In *IFAC Conference on Analysis and Design of Hybrid Systems*.
- Basiri, M., Bishop, A. N., & Jensfelt, P. (2010). Distributed control of triangular formations with angle-only constraints. *Systems & Control Letters*, 59, 147–154.
- Cao, M., Yu, C., & Anderson, B. D. (2011). Formation control using range-only measurements. *Automatica*, 47, 776–781.
- Cao, Y., & Ren, W. (2009). Containment control with multiple stationary or dynamic leaders under a directed interaction graph. In *Proceedings of the 48th IEEE Conference on Decision and Control and 28th Chinese Control Conference*. (pp. 3014–3019).
- Coogan, S., Arcak, M., & Egerstedt, M. (2011). Scaling the size of a multiagent formation via distributed feedback. In *Proceedings of the 50th IEEE Conference on Decision and Control and European Control Conference* (pp. 994–999).
- Desai, J., Ostrowski, J., & Kumar, V. (1998). Controlling formations of multiple mobile robots. In *IEEE International Conference on Robotics and Automation* (pp. 2864–2869).
- Eren, T. (2007). Using angle of arrival (bearing) information for localization in robot networks. *Turkish Journal of Electrical Engineering & Computer Sciences*, 15, 169–186.
- Eren, T., Anderson, B. D. O., Morse, A. S., Whiteley, W., & Belhumeur, P. B. (2004). Operations on rigid formations of autonomous agents. *Communications in Information and Systems*, (pp. 223–258).
- Fax, J., & Murray, R. (2004). Information flow and cooperative control of vehicle formations. *IEEE Transactions on Automatic Control*, 49, 1465–1476.
- Hendrickx, J. M., Anderson, B. D. O., Delvenne, J.-C., & Blondel, V. D. (2007). Directed graphs for the anal-

- ysis of rigidity and persistence in autonomous agent systems. *International Journal of Robust Nonlinear Control*, *17*, 960–981.
- Jadbabaie, A., Lin, J., & Morse, A. S. (2003). Coordination of groups of mobile autonomous agents using nearest neighbor rules. *IEEE Transactions on Automatic Control*, *48*, 988–1001.
- Khalil, H. K. (2002). *Nonlinear Systems*. (3rd ed.). Prentice Hall.
- Krick, L., Broucke, M., & Francis, B. (2008). Stabilization of infinitesimally rigid formations of multi-robot networks. In *Proceedings of the 47th IEEE Conference on Decision and Control, 2008*. (pp. 477–482).
- Lawton, J., Beard, R., & Young, B. (2003). A decentralized approach to formation maneuvers. *IEEE Transactions on Robotics and Automation*, *19*, 933–941.
- Ogren, P., Fiorelli, E., & Leonard, N. E. (2004). Cooperative control of mobile sensor networks: Adaptive gradient climbing in a distributed environment. *IEEE Transactions on Automatic Control*, *49*, 1292–1302.
- Oh, K.-K., & Ahn, H.-S. (2010). A survey of formation of mobile agents. In *2010 IEEE International Symposium on Intelligent Control* (pp. 1470–1475).
- Olfati-Saber, R., Fax, J. A., & Murray, R. M. (2007). Consensus and cooperation in networked multi-agent systems. *Proceedings of the IEEE*, *95*, 215–233.
- Olfati-Saber, R., & Murray, R. (2004). Consensus problems in networks of agents with switching topology and time-delays. *IEEE Transactions on Automatic Control*, *49*, 1520–1533.
- Ren, W., & Beard, R. (2005). Consensus seeking in multiagent systems under dynamically changing interaction topologies. *IEEE Transactions on Automatic Control*, *50*, 655–661.
- Reynolds, C. (1987). Flocks, herds, and schools: A distributed behavioral model. In *SIGGRAPH '87 Conference Proceedings* (pp. 25–34).
- Sastry, S. (1999). *Nonlinear Systems*. Springer.
- Sepulchre, R., Paley, D., & Leonard, N. (2008). Stabilization of planar collective motion with limited communication. *IEEE Transactions on Automatic Control*, *53*, 706–719.
- Servatius, B., & Whiteley, W. (1999). Constraining plane configurations in CAD: Combinatorics of lengths and directions. *SIAM Journal on Discrete Mathematics*, *12*, 136–153.
- Shi, G., & Hong, Y. (2009). Global target aggregation and state agreement of nonlinear multi-agent systems with switching topologies. *Automatica*, *45*, 1165–1175.
- Sontag, E. (1989). Smooth stabilization implies coprime factorization. *IEEE Transactions on Automatic Control*, *34*, 435–443.
- Tanner, H., Jadbabaie, A., & Pappas, G. (2003). Stable flocking of mobile agents, part I: Fixed topology. In *Proceedings of the 42nd IEEE Conference on Decision and Control, 2003*. (pp. 2010–2015).
- Tanner, H., Pappas, G., & Kumar, V. (2004). Leader-to-formation stability. *IEEE Transactions on Robotics and Automation*, *20*, 443–455.
- Tsitsiklis, J., Bertsekas, D., & Athans, M. (1986). Distributed asynchronous deterministic and stochastic gradient optimization algorithms. *IEEE Transactions on Automatic Control*, *31*, 803–812.
- Vicsek, T., Czirok, A., Ben-Jacob, E., Cohen, I., & Shochet, O. (1995). Novel type of phase transition in a system of self-driven particles. *Physical Review Letters*, *75*, 1226–1229.
- Yu, W., Chen, G., & Cao, M. (2010). Some necessary and sufficient conditions for second-order consensus in multi-agent dynamical systems. *Automatica*, *46*, 1089–1095.